DOI: 10.31276/VJSTE.2024.0023

Tensile strength and elongation prediction for pulsed current gas tungsten arc welded AISI 4135 steel by auto-associative memory network

Efezino McCarthy Elutabe[1], Sunday Ayoola Oke[1*], John Rajan[2], Swaminathan Jose[3]

[1]Department of Mechanical Engineering, University of Lagos, Lagos, Nigeria
[2]School of Mechanical Engineering, Vellore Institute of Technology, Chennai Campus, India
[3]School of Mechanical Engineering, Vellore Institute of Technology, Vellore, India

Received 6 January 2024; revised 12 March 2024; accepted 25 April 2024

Abstract:

This study predicts the tensile strength and elongation of pulsed current gas tungsten arc welding (PCGTAW) of AISI 4135 P/M steel welds using an auto-associative memory network. The parameters investigated include gas flow rate, base current, welding speed, and peak current. The outcomes measured were tensile strength and percentage elongation. The implementation of the auto-associative memory network was conducted using Python 3.5 on Google Colab. The network's patterns ranged from 1 to 9, with optimal weights varying from 1.0000e+00 to -1.8414e-14 and a prediction accuracy of 100%. The original data patterns stored and recalled by the network showed an all-yes connect recall status. The results demonstrated that a simple auto-associative memory network of two layers can store and recall PCGTAW process data. The mean absolute error and root mean square error between the predicted and actual tensile strength were 37.13 and 46.83 MPa, respectively, and for elongation percentage, they were 0.64 and 0.91%, respectively. This study contributes to the understanding of tensile and elongation characteristics of welded AISI 4135 steel using gas tungsten arc welding and a predictive model.

Keywords: **arc welding, artificial neural network, prediction, welding.**

Classification numbers: **2.1, 2.3**

1. Introduction

The prediction of tensile strength and elongation in the PCGTAW process for AISI 4135 P/M steel welds is crucial. Inadequate predictions can hinder productivity and increase material wastage. With the expanding scope of welding enterprises and researchers' efforts to support decision-makers, various predictive methods have been employed in recent years [1-6]. For example, S. Sirohi, et al. (2023) [7] analysed the tensile failure of Inconel 617 alloy during gas tungsten arc welding (GTAW) and compared it with shielded metal arc welding (SMAW), finding that failure occurred at the weld zone with tensile strength values near that of the base metal. The measured tensile strength values were 766±22, 570±5, 760±7, and 600±8 MPa for the respective processes of GTAW-RT, GTAW-HT, SMAW-RT and SMAW-HT.

G. Dak, et al. (2023a) [8] employed the GTAW method to predict tensile failure in P92 creep strength-enhanced ferritic steel and 304L austenitic stainless steel joints, reporting a decline of 381 MPa in tensile strength. Further studies by G. Dak, et al. (2023b) [9] showed distinct outcomes when P92 steel was buttered with IN82 material, with tensile specimens failing at the base material (AISI 304L) at a tensile strength of 404 MPa, compared to 307 MPa for P92 steel at temperatures of 550 and 650°C, respectively.

Additionally, R. Kumar, et al. (2023a) [10] predicted temperature fields and residual stresses using a comparison of hotwire-based and conventional GTAW in deep hole drilling, validated using ABAQUS software. A.K. Maurya, et al. (2024) [11] predicted the tribological performance of GTAW operations with SDSS 2507/IN-625 joints in marine applications, finding superior performance with filler ERNiCrMo-3 compared to ER2594 under increased slurry concentration. While the SDSS 2507bm had 1.45 times faster erosion when the slurry concentration increased, the IN-625 BM experienced 1.8 times faster as the slurry concentration increased.

*Corresponding author: Email: sa_oke@yahoo.com

CC BY NC ND
Crossref Similarity Check Powered by iThenticate

These research activities have diversified the network predictive methods available to assist businesses significantly. Given the importance of a network's ability to recall experimental data, choosing an appropriate memory-based network is critical. Consequently, this study supports welding operations by predicting tensile strength and percentage elongation of a novel process called pulse current gas tungsten arc welding (PCGTAW) process for the AISI 4135 steel welds using the auto-associative memory network (AMN).

Arc welding processes like gas tungsten arc welding (GTAW) and gas metal arc welding (GMAW) are widely used in joining steel parts across various industries [12-17]. Among these, the PC-GTAW process offers advantages such as low heat input. The most important parameters for this process are gas flow rate, peak current, welding speed, and base current. Furthermore, the uniqueness of the PCGTAW process and the mechanism of the auto-associative memory network need to be highlighted. Tungsten's use in the process improves efficiency as it is non-consumable, and the inert gas prevents corrosion and undesired reactions. Next are the uniqueness and the mechanism of the auto-associative memory network. The auto-associative memory network stores patterns mimicking the human mind. It encodes patterns in its neurons and recalls them when fed into the network, demonstrating its memory capability.

The motivation for this study is derived from the critical need to predict the tensile strength and percentage elongation of the PCGTAW process for AISI 4135 P/M steel welds. Inadequate prediction of these outcomes can hinder productivity and increase material wastage during the welding process. Therefore, the purpose of this study is to predict the strength and elongation of the PCGTAW process parameters, modelled as data patterns using an auto-associative memory network.

Memory is a psychological process involving the acquisition, storage, retention, and retrieval of information. In the context of welding, data from highly complex industrial processes needs to be recalled periodically. Understanding past welding activities is essential for framing the present and predicting future welding behaviours. This necessity underscores the importance of a predictive model with robust memory capabilities. The auto-associative memory network, a version of the neural network, applies this concept to the AISI 4135 steel welds in this study. This highlights the importance of investigating the predictive and recall attributes of the auto-associative memory network for AISI 4135 steel welds. Additionally, understanding the relative importance of each parameter and their comparative performance is crucial for studying their predictive attributes in the context of AISI 4135 steel.

This article contributes to the growing literature on the prediction of material properties by proposing a potential route to enhance decision-making in welding processes. It examines the tensile strength and elongation of AISI 4135 steel in the PCGTAW process using an auto-associative memory network. Previous relevant literature on material property prediction has primarily focused on mechanical properties from various parametric viewpoints. For example, A. Bahrami, et al. (2005a) [18] studied the room-temperature mechanical characteristics of dual-phase steel, considering parameters such as the morphology of martensite, deformation temperature, pre-strain, and volume fraction using a neural network model. Others have focused on flow stress prediction using artificial neural networks [19]. However, these studies largely concentrated on compression and deformation processes, with joint welding using the GTAW process often overlooked. Where the process has been used (e.g., [20, 21]), prediction using a neural network is entirely absent.

By employing an auto-associative memory neural network model and focusing on the tensile strength and elongation properties of AISI 4135 steel, this study not only responds to calls within the literature for exploring applications beyond the commonly used backpropagation method but also addresses the need to predict outside the deformation and compressive processes. This approach highlights the need for a fresh understanding of AISI 4135 steel in decision-making processes for joint materials in the GTAW process.

2. Literature review

A literature search yielded 50 relevant sources on using artificial neural networks (ANNs) in welding. These were grouped into five themes and explained in Table 1:

Table 1. Summary of the literature review.

S/No.	Source	Parameters	Output	Application area	Method used	Limitations	Results found
Paper group 1: Studies that predict the weld penetration and weld geometry							
1	[22]	Reflected laser pattern image	Weld penetration	Weld control & optimisation in the manufacturing Industry	Deep convolutional neural network (DCNN), saliency map	Inability to predict the strength of the resulting weld	98.1% accuracy was achieved and indicates a high correlation existing between the pool surface and weld penetration
2	[23]	Welding current and voltage	Welding quality	Weld control & optimisation in the manufacturing Industry	Deep learning model	The paper only proposes a pipeline but does not apply it. Nor does the paper specify what characteristics it intends to measure as welding quality	A proposal of a four-phase pipeline to leverage common inputs to determine welding quality was made
3	[2]	Weld pool image	Weld penetration	Weld control & optimisation in the manufacturing Industry	Enhanced deep random forest fusion method	Cannot determine the strengths of the resulting welds	The method can use limited data to determine the weld penetration and is comparable with the best machine learning algorithms
4	[5]	Arc sound	Penetration state	Weld control & optimisation in the manufacturing Industry	Squeeze and excitation network, convolutional neural network.	Inability to determine the weld defects and the resulting strength of the weld	98.25% accuracy and outperforms other models as confirmed by experimental setups
Paper group 2: Investigations on the prediction of weld strength							
5	[24]	Laser power, scan speed, frequency, duty factor, and focal positions	Bead area, micro-hardness, and tensile strength	Weld control & optimisation in the manufacturing Industry	Artificial neural network	The best network architecture for the task at hand is not investigated	The artificial neural network can be used to determine the weld characteristics for both forward and reverse models
6	[25]	Pulse duration, voltage (pulse, background), welding speed, wire feed rate, welding current, welding voltage	Ultimate tensile strength	Weld optimisation in the manufacturing Industry	Multiple regression method, artificial neural networks (ANNs)	Inability to determine what parameters need to change in real-time to obtain the best weld strength	Artificial neural network is more accurate in prediction than Multiple linear regression
7	[26]	Inert gas flow rate, voltage and welding current	Tensile Strength, Weld hardness	Weld control & optimisation in the manufacturing Industry	Artificial neural networks (ANNs), genetic algorithms (GAs)	Computational time required for real-time control of a weld	Hybrid genetic algorithm-artificial neural network method showed more accuracy than the traditional surface response methodology with an error of approximately 5%
8	[27]	Pipe radius to thickness ratio, the thickness, the heat input, and the normalised through-thickness position.	Hoop and axial residual stress in the weld centre line (WCL)	Weld control & optimisation in the manufacturing Industry	Artificial neural network (ANN) models	Inability to predict both hoop and axial stresses using one neural network	Accurate prediction of stresses with root mean square error (RMSE) for the axial and hoop stress ANN models was respectively 69 and 89 MPa
Paper group 3: Articles on the prediction and detection of weld defects							

S/No.	Source	Parameters	Output	Application area	Method used	Limitations	Results found
9	[28]	Weld image	Under penetration, full penetration, burning through	Weld control & optimisation in the manufacturing Industry	Convolutional neural network	Inability to determine the strengths of welds that are not defective	Accuracy of 99.38% based on real-time weld images
10	[4]	Top surface image	Weld quality: weld penetration, burn through	Weld control & optimisation in the manufacturing Industry	Convolutional neural network	Inability to detect defects as well as the resulting strength of the weld	Can predict weld penetration and excessive burn-through within 1mm error with 95% accuracy
11	[29]	Current, voltage, travel speed, and contact tube to workpiece distance (CTWD)	Presence of defects: porosity, lack of penetration and burn-through	Weld control & optimisation in the manufacturing Industry	Decision tree, support vector machine	The ability of neural networks to perform the same classification is not investigated and compared	Both models proposed (SVM, and decision tree) are suitable for identifying the defects.
12	[3]	Weld current and weld voltage	Angular distortion	Weld control & optimisation in the manufacturing Industry	Back propagation neural network	Inability to determine the weld defects and the resulting strength of the weld	Accurate prediction of angular distortion by the method proposed
Paper group 4: Research that optimises and controls weld processes							
13	[30]	Arc current, torch travel speed, and filler wire feed rate	Plate thickness, updated input parameters	Weld control & optimisation in the manufacturing Industry	Feedforward, sensor-enabled, arc process control	Inability to predict the strength of the weld and requirement of costly image sensors	Model can derive the plate thickness as well as determine the required process parameters for welding control with a latency low enough to ensure continuous welding
14	[31]	Top side weld bead geometry	Weld back side bead width	Weld control & optimisation in the manufacturing industry	Convolutional neural network, multi-layer perceptron and a gradient descent algorithm	Inability to predict the occurrence of defects or the resulting strength of the weld	Real-time prediction and optimisation are attainable with the models developed as verified by experimental studies
Paper group 5: Reports that evaluate other papers and their prediction/optimisation methods							
15	[32]	Weld seam and weld pool image	Welding dimensions and quality required	Advanced welding manufacturing	Survey on and review of other research papers	The existence of predictors of the weld pool and weld seam which do not need costly sensors are not examined.	The weld seam and weld pool are the most important information sources for real-time sensing in determining what adjustments need to be made while welding
16	[33]	Welding current, welding speed, feed rate and arc length	Bead geometries, reinforcement, and weld deposition	Gas tungsten arc welding research	Survey on and review of other research papers	Relationship between what parameters affect certain outputs is not investigated.	The prediction of strength and corrosion require more research
17	[34]	Gap, current, voltage and speed	Weld bead width	Weld control & optimisation in the manufacturing Industry	Neural network and multiple regression model	Inability to predict the tensile strength of the resulting weld and to check if it conforms to industry standards	Both models more accurately predict the weld bead width than the weld bead depth
18	[35]	Welding speed, welding voltage, and heat source moving speed	Weld bead geometry	Weld control & optimisation in the manufacturing Industry	Artificial neural network (ANN) and a multiple linear regression (MLR) model	Inability to predict the occurrence of defects or the tensile strength of the weld	ANN model performs better than the MLR model. There is an excellent match when compared with experimental results

1. Studies predicting weld penetration and geometry

2. Investigations on predicting weld strength

3. Articles on predicting and detecting weld defects

4. Research optimising and controlling weld processes

5. Reviews evaluating other papers and their prediction/ optimisation methods

The main observations from the literature study are as follows:

• Predicted weld strength is typically based on stress, including TS, impact strength, hardness, micro-hardness, nominal shear strength, hoop and axial stress, residual stress, and elongation (used to evaluate quality alongside strength).

• Models predicting or detecting weld defects are highly reliant on the nature of the arc produced. The input is captured in various forms such as arc sound, arc spectral signal (spectral bands/lines), and arc image.

• In addition to speed, current, and voltage, the geometry of the weld pool is the most important parameter in optimising and controlling weld processes. This geometry is usually fed as input to the models in the form of weld pool images, top side bead width (TSBW), and top surface height.

The major research gap identified across all groups is the lack of publicly released data for the community to verify and extend researchers' claims after publication. This absence of shared data makes it challenging for other researchers to improve their models.

3. Materials and methods

3.1. Experiment, materials and equipment

In a subsequent section of this article, the results of experiments discussed in the present work will be utilised to analyse the method presented. However, the experiments were previously conducted and presented by J. Joseph, et al. (2016) [36]. Thus, no new experiments have been conducted in the present study; only an elaboration of the study by J. Joseph, et al. (2016) [36] is provided here.

To start with, J. Joseph, et al. (2016) [36] experimented on the PCGTAW, involving the generation of coalescence through heating the workpiece using an electric arc placed between the tungsten electrode and the base metal. First, the iron powder was sourced in particle form, approximately 150 micrometres in size. The use of iron powder was intended to enhance metal recovery by adding it to the metal alloy. Additionally, the electrode coating was diluted with iron powder to efficiently utilise the heat generated during welding. Green compacts of the powder blend were made and ceramic coating was applied to the surfaces of the green compacts to prevent oxidation during sintering. The experiment involved maintaining the coated compacts at a temperature range of 1140-1160°C for 1.5 h in an electric muffle furnace. Flat plates with dimensions of 150x55x5 mm were then produced as the forged products. The furnace was cooled to room temperature [36]. Machining was performed on the surfaces of the flat plates, resulting in a preform with dimensions of 150x50x3 mm. Pulse current gas welding was then performed on the sample AISI 4135 steel.

It is worth noting that the above experiments were extracted from J. Joseph, et al. (2016) [36]. The materials used for the experiment included tensile specimens and weld plates, among others. The equipment used included an electric muffle furnace.

3.2. Computational methods

The simplest structure of an auto-associative memory network (AMN) that can be used for storing and predicting patterns is a two-layered AMN where both layers serve as input and output, and the patterns are stored in the weights, as shown in Fig. 1 [37].

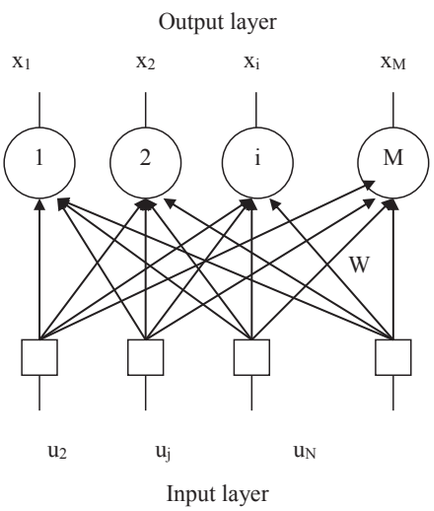

Fig. 1. The auto-associative memory network structure.

Here, the input layer (u_i) is at the bottom and the output layer (x_i or x^k) is at the top, both of which are connected by a set of weights (W_{ij}). W_{ij} represents the value of the weight that connects input neuron (u_j) to output neuron (x_i) [36]. This AMN structure will be used in this paper to store and predict PCGTAW patterns (i.e., parameters, strength, and quality of the weld) as it can store patterns in the form of vectors. The outputs can be represented in the form of the inputs and the weights via Eqs. (1) and (2) [18, 37].

$$x_i = W_{ij}\, u_j \quad (1)$$

$$x^K = W^T u^K \quad (2)$$

Given that the neural network structure has only two layers, the relationship between the output and the input captured in Eq. (1) can be represented in matrix format as shown in Eq. (2). The optimisation of the weights (W^T) can then be calculated using a linear algebra relation that minimises the difference between the desired output (u^K) and the calculated output of the network (y^K). In other words, the optimised weight can be calculated using the expression shown in Eq. (3) [37]:

$$A^* = \min | y^K - Au^K | \quad (3)$$

where A is any weight set and A^* is a specific weight set that satisfies the minimum expression. A^* can then be calculated using the pseudo-inverse method as shown in Eqs. (4) and (5) [37]:

$$A^* = \mathrm{Y}U^+ \quad (4)$$

$$U^+ = (U^T U)^{-1} U^T \quad (5)$$

where U is the matrix representation of u^K, Y is the matrix representation of y^K, U^+ is the pseudoinverse of U, U^T is the transpose of U, and $(U^T U)^{-1}$ is the matrix inverse of $U^T U$.

Once W^T has been calculated, the optimal set of weights for the patterns to be stored has been acquired, and we can now use Eq. (2) for the AMN in conjunction with Eq. (6) [37]:

$$W^T = A^* \quad (6)$$

It is important to note that when using the AMN, it is necessary to normalise the input patterns to prevent numbers from scaling up to infinity as they get multiplied in the neural network. However, this also encodes the patterns, so it is necessary to add a key to the input to help decode the output of the network. The entire process flow of this implementation is shown in Fig. 2.

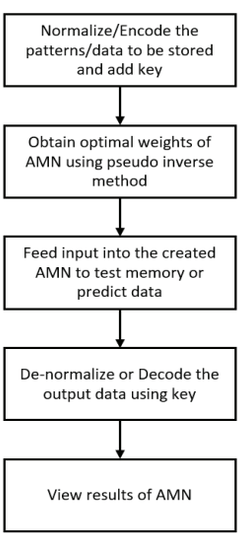

Fig. 2. Auto-associative memory network implementation process flow.

The implementation process of the AMN is carried out using Python 3.5 on Google Colab's Notebook.

4. Results and discussion

This section discusses the application of AMNs, which are feed-forward networks. In this context, data on welding speed, peak current, base current, and gas flow rate are used as inputs, with tensile strength and percentage elongation as responses. These inputs are entered through the input nodes, each representing the aforementioned parameters. The feed-forward nature describes how the welding data travels through the hidden layers and is subsequently ejected through the output nodes. The hidden layers of the AMN method are critical components that facilitate the handling of complex neural networks. Their main functions in processing the welding data include transformation and the development of automotive attributes.

To further describe the AMN as a feed-forward network, it is designed to avoid situations where welding information loops back to the outputs. By preventing this, the welding data feed-forward network produces approximate functions, which represent the identities of the mapped data from the input sections to the outputs. In summary, the researchers used the AMN method to store and predict the data shown in Table 2.

Table 2. Working range of pulsed current gas tungsten arc welding parameters used by J. Joseph, et al. (2016) [36].

Parameters	Notation	Level		
		1	*2*	*3*
Peak current	I_p/A	60	70	80
Base current	I_b/A	30	35	40
Welding speed	WS/(mm/min)	60	70	80
Gas flow rate	GFR/lpm	8	10	12

To achieve this goal, the researchers divided the AMN structure into layers: the input layer and the output layer. The input layer serves as the gateway for receiving and processing welding information from the experimental data collected by J. Joseph, et al. (2016) [36]. This layer is represented by four artificial neurons (nodes). The output layer, which is the final layer of the AMN, indicates the values of the welding response predictions, used for welding decision-making. Since two welding responses are being predicted in this study, namely the tensile strength and percentage elongation of the AISI 4135 steel welds, the output layer comprises two nodes, each representing one of

these responses. The outputs exhibit a set of weights and biases that get activated before yielding the final outputs. The network developed for welding elemental prediction is referred to as a densely connected network, where every input node is connected to every hidden layer node, and each hidden layer node is connected to the output layer. This connectivity is achieved through a set of weights (w_i).

To store the data in the AMN method, the researchers calculated the weights using the pseudoinverse method. The pseudoinverse aims to evaluate the "best fit" solution for a set of linear equations formulated based on the inputs and outputs of the welding system. Although these equations lack a direct solution, the pseudoinverse provides the minimum norm solution where multiple solutions exist. The pseudoinverse mechanism involves computing the reciprocal for each non-zero element along the matrix diagonal, leaving zeros unchanged, and then transposing the matrix. The pseudoinverse expression is given in Eqs. (1) to (3) [37]. Here, y_k is the desired output, A is any set of weights, and U_k is the input. When the researcher obtains A such that it yields the minimum expression, it is referred to as A^*. A^* is the specific weight set that minimises the expression.

As these weights are obtained for all desired input data, the AMN possesses its memory and can store the corresponding datasets. To recall the memory, the researcher provides the model with part or all of the data and observes the network's output. If the network outputs the same data, it implies that the data is stored in its memory. This stage represents the storage aspect of the AMN method.

After building the network, it was tested for storage and prediction. For prediction, the researcher feeds part of the data into the network. If the network can accurately generate the rest of the data, it can predict the data. The memory test showed 100% accuracy, indicating the AMN could recall every stored pattern. However, for prediction, the accuracy was 14%. Analysis revealed that the network predicted a singular output regardless of the input data, likely due to the small dataset size. With a larger dataset, the network should predict more accurately.

The AMN method was implemented using Python 3.5 on Google Colab's Notebook. The process involves normalising the data to prevent numbers from scaling up to infinity. The data, including base current, peak current, welding speed, and gas flow rate, is normalised, and a key is added with a unit value of 1. The pseudoinverse method is used to calculate the optimal weights, after which the network is trained. The network works with normalised data and, upon processing, denormalises it using the key. This ensures successful decoding of the data, which is then interpreted for the AMN method. Codes are written for the inputs and outputs. By observing the memory test of the code, the input pattern for the table is noted, and information about the programme recall is also shown. The same procedure applies to the prediction test.

Each row of Table 3 is fed into the AMN implementation process as a pattern to be stored, so the AMN will use them as a base memory for predicting other patterns. The key used to encode and decode the patterns is the addition of a unit value to each row. When the output pattern is obtained, the pattern is decoded/denormalised to ensure the key added has a unit value of 1. Table 4 shows the patterns fed into the AMN, and Table 5 shows the optimal weights obtained.

Table 3. Experimental results [36].

Expt. no	Actual value				Tensile strength (MPa)	% of elongation
	I_p/A	I_b/A	*WS/(mm/min)*	*GFR/lpm*		
1	60	30	60	8	630	8.65
2	60	35	70	10	609	8.95
3	60	40	80	12	595	9.05
4	70	30	70	12	642	9.37
5	70	35	80	8	558	6.15
6	70	40	60	10	665	8.58
7	80	30	80	10	581	8.14
8	80	35	60	12	718	8.50
9	80	40	70	8	610	7.90

Table 4. Patterns fed into the auto-associative memory network.

Pattern no.	I_p/A	I_b/A	WS/(mm/min)	GFR/lpm	Tensile strength (MPa)	% of elongation	Key
Pattern 1	60	30	60	8	630	8.65	1
Pattern 2	60	35	70	10	609	8.95	1
Pattern 3	60	40	80	12	595	9.05	1
Pattern 4	70	30	70	12	642	9.37	1
Pattern 5	70	35	80	8	558	6.15	1
Pattern 6	70	40	60	10	665	8.58	1
Pattern 7	80	30	80	10	581	8.14	1
Pattern 8	80	35	60	12	718	8.50	1
Pattern 9	80	40	70	8	610	7.90	1

Table 5. Optimal weights generated by auto-associative memory network.

1.0000e+00	2.0615e-12	4.5215e-12	7.5462e-13	4.1941e-11	5.2650e-13	6.7574e-14
1.5778e-11	1.0000e+00	1.6292e-11	2.3311e-12	1.4179e-10	1.9005e-12	2.2977e-13
-4.3718e-12	-2.1317e-12	1.0000e+00	-1.4812e-12	-6.4792e-11	-6.6801e-13	-1.0779e-13
8.4708e-12	4.1501e-12	1.4945e-11	1.0000e+00	1.5691e-10	1.4458e-12	2.6208e-13
-6.3493e-13	-3.2812e-13	-1.0853e-12	-2.6971e-13	1.0000e+00	-1.0811e-13	-1.8414e-14
-1.8647e-12	-9.6434e-13	-5.2108e-12	-1.5995e-12	-5.9160e-11	1.0000e+00	-1.0174e-13
2.2441e-10	1.0322e-10	5.5138e-10	1.7115e-10	6.2684e-09	5.0961e-11	1.0000e+00

Given the optimal weights, two tests were carried out on the AMN: A memory test and a prediction test.

4.1. Memory test

In the memory test, the same input patterns are fed into the AMN to check whether the AMN will remember the data. This test is shown in Table 6. The accuracy of the AMN on the memory test is defined as shown in Eq. (7):

Accuracy = Number of correctly reconstructed patterns/Number of total patterns stored (7)

Table 6. Memory test of the created auto-associative memory network method.

Original data pattern stored in the auto-associative memory network	Data pattern recalled by auto-associative memory network	Correct recall
[60. 30. 60. 8. 630. 8.65]	[60. 30. 60. 8. 630. 8.65]	Yes
[60. 35. 70. 10. 609. 8.95]	[60. 35. 70. 10. 609. 8.95]	Yes
[70. 30. 70. 12. 642. 9.37]	[70. 30. 70. 12. 642. 9.37]	Yes
[70. 35. 80. 8. 558. 6.15]	[70. 35. 80. 8. 558. 6.15]	Yes
[70. 40. 60. 10. 665. 8.58]	[70. 40. 60. 10. 665. 8.58]	Yes
[80. 30. 80. 10. 581. 8.14]	[80. 30. 80. 10. 581. 8.14]	Yes
[80. 35. 60. 12. 718. 8.5]	[80. 35. 60. 12. 718. 8.5]	Yes
[80. 40. 70. 8. 610. 7.9]	[80. 40. 70. 8. 610. 7.9]	Yes

From Table 6 and Eq. (7):

Accuracy = 8/8 = 100%

Therefore, the memory accuracy of the AMN is 100%. This implies that the AMN can recall every pattern stored in it.

4.2. Prediction test

In the prediction test, the same input patterns are fed into the AMN, but the tensile strength and percentage elongation values are set to the average of the initially stored patterns. The accuracy of the AMN on the prediction test is determined by the average percentage deviation of the predicted values from the actual values, as expressed in Eq. (8):

$$\text{Accuracy} = \frac{1}{N}\sum_{i=1}^{N}\left(\frac{|\,p_i - o_i\,|}{|\,o_i\,|}\right) \quad (8)$$

where p_i is the predicted value of item i, o_i is the original value in the pattern i, and N is the number of prediction tests conducted.

Table 7. Prediction test of the created auto-associative memory network.

Actual strength and elongation	Predicted strength and elongation	Pattern no. (i.e., the value of *i*)
[630. 8.65]	[623.1111 8.3656]	[1 2]
[609. 8.95]	[623.1111 8.3656]	[3 4]
[642. 9.37]	[623.1111 8.3656]	[5 6]
[558. 6.15]	[623.1111 8.3656]	[7 8]
[665. 8.58]	[623.1111 8.3656]	[9 10]
[581. 8.14]	[623.1111 8.3656]	[11 12]
[718. 8.5]	[623.1111 8.3656]	[13 14]
[610. 7.9]	[623.1111 8.3656]	[15 16]

Using Eq. (8) and Table 7, the prediction accuracy is 14.28%. This means the AMN created is currently incapable of accurately predicting the strength and elongation patterns, likely due to the small dataset used for training. The mean absolute error and the root mean square error between the predicted and actual tensile strength are 37.13 and 46.83 MPa, respectively, and for elongation percentage, they are 0.64 and 0.91%, respectively.

4.3. Limitations and advantages of the proposed method

One noticeable development when applying the auto-associative memory network method is that the pseudoinverse method, used to optimise outputs from the inputs, often returns the identity matrix or its approximation as the weight set. This is expected because the memory network is trained to recall the inputs as outputs. No other weight set would perform better than the identity matrix. However, the identity matrix merely reflects the inputs, similar to a mirror, and does not infer from the data. This leads to a false memory, which is why the method excels in the recall test but fails in the prediction test. When trained with partial data, it does not return the identity matrix,

and it performs better in prediction compared to the auto-associative memory network. However, the network fails the prediction test. When trained on partial data, the identity matrix is not returned. It excels in prediction compared to the auto-associative memory network. In light of this, future studies may attempt to add another method that boosts prediction and overcomes this mentioned weakness.

Moreover, the backpropagation ANNs are the most prevalent method used in science against the auto-associative memory artificial network proposed in this study for predicting the tensile strength and elongation of the AISI 4135 steel used in GTAW. In the auto-associative method, an attempt is made to replicate the same inputs as outputs. It encodes the data into its weights, and if given partial data, it can complete the data generation. However, backpropagation does not encode the data into its weight but optimises its weights to yield the correct output data when given input data.

For example, suppose we have four parameters A, B, C, and D. The auto-associative method works by creating four neurons A, B, C, and D and connecting them in any manner in the hidden layers to output another four neurons predicting A, B, C, and D. If the network is given different inputs, say A, B, and C, to predict D, it can also predict the last one as A. Given any two inputs, the auto-associative method can complete the prediction. For backpropagation, if the researcher works with four neurons A, B, C, and D, the method predicts another output, E. Partial data can be fed into the auto-associative method, and it will complete the result since it has stored the data in its memory weights.

The weakness of the auto-associative method lies in its limited memory capacity. It can only store a limited number of data patterns and retrieve them upon query. However, backpropagation does not need to store many data points as it functions directly. The limit of backpropagation might be in the correctness of the output, while the auto-associative method's recall accuracy is known to be correct or close to the desired results. The correctness of backpropagation results depends on the accuracy obtained during computations, or the root mean squared error used for accuracy computation. Another difference between backpropagation and the auto-associative network is that the latter is symmetrical while the former is not. The auto-associative method is symmetrical because the input data should match the output result.

In terms of flexibility, the backpropagation neural network is more flexible than the auto-associative memory network. Flexibility depends on the number of neurons or rates needed for each method to work adequately. The auto-associative neural network requires more weights and neurons to process input data patterns. If a certain minimum is not met, it will not store as much data as required. However, the backpropagation neural network can use a relatively small number of neurons and input data. As the number of weights increases, performance improves. Nonetheless, one is not limited by the number of weights or neurons that should be used.

4.4. Novelty and application of work

The novelty of this study lies in the prediction of tensile strength and elongation of the AISI 4135 steel material using an innovative method called the AMN method. Previously, J. Joseph, et al. (2016) [36] conducted experiments on the AISI 4135 steel material and obtained experimental results for tensile strength and elongation. They also predicted these two characteristics using a genetic algorithm and simulated annealing, obtaining values of 693.62 MPa and 8.21% elongation with the genetic algorithm, and 685.31 MPa and 8.29% elongation with simulated annealing. In contrast, our prediction using the AMN method was 623.11 MPa for tensile strength and 8.37% for elongation, which is much closer to the experimental data, demonstrating the uniqueness and accuracy of the AMN method. The process parameters were analysed using advanced machine learning techniques implemented with Python. Distinct patterns were created to observe the optimal weights during the evaluation process. From a prediction standpoint, the AMN method exhibits competitive attributes compared to other methods, using memory and productive characteristics to enhance the accuracy of parametric performance predictions.

The application of the AMN method to the AISI 4135 material offers a wide range of applications to assist welding engineers. By using data and procedures, the AMN method mimics how engineers learn from past data to enhance prediction accuracy. The AISI 4135 material is useful for shafts (found in motor vehicle construction, particularly for engines and transmissions). It is also widely used in forging for valves, fittings, and oil industry applications, as well as in high-pressure steel cylinders for various uses with gases and pressurised liquids.

5. Conclusions

In this article, the tensile strength and percentage elongation of AISI 4135 steel welds were estimated using base current, gas flow rate, welding speed, and peak current as inputs. The investigation led to the following conclusions:

1. The tensile strength and percentage elongation can be accurately estimated using the auto-associative memory network method, avoiding the time-consuming and costly experimental testing methods.

2. The mean absolute error and the root mean square error between the predicted and actual tensile strength are 37.13 and 46.83 MPa, respectively. For elongation percentage, they are 0.64 and 0.91%, respectively.

The Python code used for this method can be adjusted to study other parameters that significantly influence tensile strength and percentage elongation. Although this study used tensile strength and percentage elongation to analyse the material responses, future work could examine fracture surfaces using metrics developed from scanning electron microscopy (SEM) images, which the AMN model could predict based on input parameters. Additionally, using extended orthogonal arrays such as L27 instead of the restricted L9 used in the present analysis could produce more reliable data predictions.

Moreover, this study considered only four parameters based on the experiments conducted by J. Joseph, et al. (2016) [36]. Future studies may extend the number of parameters used to establish the process outcomes more comprehensively. Testing alternative materials to AISI 4135 steel is also recommended for future research.

CRediT author statement

Efezino McCarthy Elutabe: Conceptualisation and Methodology, Writing - Original draft preparation; Sunday Ayoola Oke: Conceptualisation and Methodology, Writing - Original and final draft preparations; John Rajan, Swaminathan Jose: Methodology and Editing.

COMPETING INTERESTS

The authors declare that there is no conflict of interest regarding the publication of this article.

REFERENCES

[1] H.T. Hoseini, M. Farahani, M. Sohrabian (2017), "Process analysis of resistance spot welding on the Inconel alloy 625 using artificial neural network", *International Journal of Manufacturing Research*, **12(4)**, pp.444-460, DOI: 10.1504/IJMR.2017.088398.

[2] D. Wu, M. Hu, Y. Huang, et al. (2021), "*In situ* monitoring and penetration prediction of plasma arc welding based on welder intelligence-enhanced deep random forest fusion", *Journal of Manufacturing Processes*, **66**, pp.153-165, DOI: 10.1016/j.jmapro.2021.04.007.

[3] C.R. Ramirez, D.F. Giarolla, J.E. Mazzaferro, et al. (2021), "Prediction of angular distortion due GMAW process of thin-sheets Hardox 450® steel by numerical model and artificial neural network", *Journal of Manufacturing Processes*, **68(A)**, pp.1202-1213, DOI: 10.1016/j.jmapro.2021.06.045.

[4] K. Nomura, K. Fukushima, T. Matsumura, et al. (2021), "Burn-through prediction and weld depth estimation by deep learning model monitoring the molten pool in gas metal arc welding with gap fluctuation", *Journal of Manufacturing Processes*, **61**, pp.590-600, DOI: 10.1016/j.jmapro.2020.10.019.

[5] Z. Zhao, R. Xiao, Q. Liu, et al. (2023), "Recognition of penetration states based on arc sound of interest using VGG-SE network during pulsed GTAW process", *Journal of Manufacturing Processes*, **87**, pp.81-96, DOI: 10.1016/j.jmapro.2022.12.034.

[6] A. Kumar, K. Guguloth, S.M. Pandey, et al. (2023), "Study on microstructure-property relationship of Inconel 617 alloy/304L SS steel dissimilar welds joints", *Metallurgical and Materials Transaction A*, **54**, pp.3844-3870, DOI: 10.1007/Sl1661-023-07136-3.

[7] S. Sirohi, N. Kumar, A. Kumar, et al. (2023), "Metallurgical characterization and high-temperature tensile failure of Inconel 617 alloy welded by GTAW and SMAW: A comparative study", *Proceedings of The Institution of Mechanical Engineers, Part L: Journal of Materials: Design and Applications*, **237(9)**, DOI: 10.1177/14644207231171266.

[8] G. Dak, K. Guguloth, A. Bhattacharyya, et al. (2023a) "Failure study of creep and high temperature tensible tested tungsten incer gas welded P92 steel and AISI 304L steel dissimilar weld joints", *Journal of Materials Engineering and Performance*, DOI: 10.1007/S11665-023-09070-2.

[9] G. Dak, V. Singh, A. Kumar, et al. (2023b), "Microstructure and mechanical behaviour study of the dissimilar weldment of 'IN82 buttered'P92 steel and AISI 304L steel for ultra super critical power plants", *Materials Today Communications*, **37**, DOI: 10.1016/j.mtcomm.2023.107552.

[10] R. Kumar, M.M. Mahapatra, A.K. Pradhan, et al. (2023), "Experimental and numerical study on the distribution of temperature field and residual stress in a multi-pass welded tube joint of Inconel 617 alloy", *International Journal of Pressure Vessel and Piping*, **206**, DOI: 10.1016/j.ijpvp.2023.105034.

[11] A.K. Maurya, W.N. Khan, A. Patriak, et al. (2024), "Tribological performance of gas tungsten arc welded dissimilar joint of SDSS 2507/IN-625 for marine application", *Archives of Civil and Mechanical Engineering*, **24(23)**, DOI: 10.1007/s43452-023-00832-2.

[12] M. Ezer, G. Cam (2022), "A study on microstructure and mechanical performance of gas metal arc welded AISI 304L joints", *Material Science and Engineering Technology*, **53(9)**, pp.1043-1052, DOI: 10.1002/mawe.202200050.

[13] M. Senol, G. Cam (2023), "Investigation into microstructures and properties of AISI 430 ferritic steel butt joints fabricated by GMAW", *International Journal of Pressure Vessels and Piping*, **202**, DOI: 10.1016/j.ijpvp.2023.104926.

[14] H.T. Serindag, G. Cam (2021), "Microstructure and mechanical properties of gas metal arc welded AISI 430/AISI 304 dissimilar stainless steels butt joints", *Journal of Physics: Conference Series*, **1777**, DOI: 10.1088/1742-6596/1777/1/012047.

[15] H.T. Serindag, G. Cam (2022a), "Multi-pass butt welding of thick AISI 316L plates by gas tungsten arc welding: Microstructural and mechanical characterization", *International Journal of Pressure Vessels and Piping*, **200**, DOI: 10.1016/j.ijpvp.2022.104842.

[16] H.T. Serindag, G. Cam (2023), "Characterizations of microstructure and properties of dissimilar AISI 316L/9Ni low alloy cryogenic steel joints fabricated by GTAW", *Journal of Materials Engineering and Performance*, **32**, pp.7039-7049, DOI: 10.1007/s11665-022-07601-x.

[17] H.T. Serindag, C. Tardu, I.O. Kircicek, et al. (2022b), "A study on microstructural and mechanical properties of gas tungsten arc welded thick cryogenic 9% Ni alloy steel butt joint", *CIRP Journal of Manufacturing Science and Technology*, **37**, pp.1-10, DOI: 10.1016/j.cirpj.2021.12.006.

[18] A. Bahrami, S.H.M. Anijdan, A. Ekrami (2005a), "Prediction of mechanical properties of DP steels using neural network model", *Journal of Alloys and Compounds*, **392(1-2)**, pp.177-182, DOI: 10.1016/j.jallcom.2004.09.014.

[19] A. Bahrami, S.H.M. Anijdan, H.R.M. Hosseini, et al. (2005b), "Effective parameters modelling in compression of an austenitic stainless steel using artificial neural network", *Computational Materials Science*, **34(4)**, pp.335-341, DOI: 10.1016/j.commatsci.205.01.006.

[20] T.R. Tabrizi, M. Sabzi, S.H.M. Anijdan, et al. (2021), "Comparing the effect of continuous and pulsed current in the GTAW process of AISI316L stainless steel welded joint: Microstructural evolution, phase equilibrium, mechanical properties and fracture mode", *Journal of Materials Research and Technology*, **15**, pp.199-212, DOI: 10.1016/j.jmrt.2021.07.154.

[21] M. Sabzi, S.H.M. Anijdan, A.R.B. Chalandar, et al. (2022), "An experimental investigation on the effect of gas tungsten arc welding current modes upon the microstructure, mechanical and fractography properties of welded joints of two grades of AISI 316L and AISI310S alloy metal sheets", *Material Science and Engineering: A*, **840**, DOI: 10.1016/j.msea.2022.142877.

[22] C. Li, J. Wang, Y. Dai, et al. (2023), "Experimental validation of saliency maps for understanding deep neural networks for weld penetration prediction", *Journal of Manufacturing Processes*, **88**, pp.22-23, DOI: 10.1016/j.jmapro.2023.01.018.

[23] Y. Hahn, R. Maack, G. Buchholz, et al. (2023), "Towards a deep learning-based online quality prediction system for welding processes", *Procedia CIRP*, **120**, pp.1047-1052, DOI: 10.1016/j.procir.2023.09.123.

[24] S. Datta, A.M. Das, M.S. Raza, et al. (2022), "Study on laser beam butt-welding of NiTinol sheet and input-output modelling using neural networks trained by metaheuristic algorithms", *Materials Today Communications*, **32**, DOI: 10.1016/j.mtcomm.2022.104089.

[25] S. Pal, S.K. Pal, A.K. Samantaray (2008), "Artificial neural network modeling of weld joint strength prediction of a pulsed metal inert gas welding process using arc signals", *Journal of Materials Processing Technology*, **202(1-3)**, pp.406-474, DOI: 10.1016/j.jmatprotec.2007.09.039.

[26] R.P. Verma, K.N. Pandey, G. Mittal (2024), "Genetic-neural optimisation approach for gas metal arc welding of dissimilar aluminium alloys of AA5083-O/AA6061-T6", *International Journal of Lightweight Materials and Manufacture*, **7(1)**, pp.214-220, DOI: 10.1016/j.ijlmm.2023.07.001.

[27] D.K. Rissaki, P.G. Benardos, G.C. Vosniakos, et al. (2023), "Residual stress prediction of arc welded austenitic pipes with artificial neural network ensemble using experimental data", *International Journal of Pressure Vessels and Piping*, **204**, DOI: 10.1016/j.ijpvp.2023.104954.

[28] Z. Zhang, G. Wen, S. Chen (2019), "Weld image deep learning-based on-line defects detection using convolutional neural networks for Al alloy in robotic arc welding", *Journal of Manufacturing Processes*, **45**, pp.208-216, DOI: 10.1016/j.jmapro.2019.06.023.

[29] S.Q. Moinuddin, S.S. Hameed, A.K. Dewangan, et al. (2021), "A study on weld defects classification in gas metal arc welding process using machine learning techniques", *Materials Today Proceedings*, **43(1)**, pp.623-628, DOI: 10.1016/j.matpr.2020.12.159.

[30] M. Vasilev, C. MacLeod, Y. Javadi, et al. (2021), "Feed forward control of welding process parameters through on-line ultrasonic thickness measurement", *Journal of Manufacturing Processes*, **64**, pp.576-584, DOI: 10.1016/j.jmapro.2021.02.005.

[31] J. Kershaw, R. Yu, Y. Zhang, et al. (2021), "Hybrid machine learning-enabled adaptive welding speed control", *Journal of Manufacturing Processes*, **71**, pp.374-383, DOI: 10.1016/j.jmapro.2021.09.023.

[32] Y. Cheng, R. Yu, Q. Zhou, et al. (2021), "Real-time sensing of gas metal arc welding process - A literature review and analysis", *Journal of Manufacturing Processes*, **70(11)**, pp.452-469, DOI: 10.1016/j.jmapro.2021.08.058.

[33] A. Karpagaraj, K. Parthiban, S. Ponmani (2020), "Optimisation techniques used in gas tungsten arc welding process - A review", *Materials Today Proceedings*, **27(3)**, pp.2187-2190, DOI: 10.1016/j.matpr.2019.09.093.

[34] J. Lee, K. Um (2000), "A comparison in a back-bead prediction of gas metal arc welding using multiple regression analysis and artificial neural network", *Optics and Lasers in Engineering*, **34(3)**, pp.149-158, DOI: 10.1016/S0143-8166(00)00097-X.

[35] R. Pradhan, A.P. Joshi, M.R. Sunny, et al. (2022), "Performance of predictive models to determine weld bead shape parameters for shielded gas metal arc welded T-joints", *Marine Structures*, **86**, DOI: 10.1016/j.marstruc.2022.103290.

[36] J. Joseph, S. Muthukumaran (2016), "Optimisation of pulsed current GTAW process parameters for sintered hot forged AISI 4135 P/M steel welds by simulated annealing and genetic algorithm", *Journal of Mechanical Science and Technology*, **30**, pp.145-155, DOI: 10.1007/s12206-015-1218-3.

[37] U. Halici (2008), *Artificial Neural Networks*, *Chapter III - Neural Networks as Associative Memory*, METU Electrical and Electronics Engineering, pp.43-58.